

Effect of ethanol on crystal growth and morphology of $\text{MgCO}_3 \cdot 3\text{H}_2\text{O}$: Based on DFT calculation and molecular dynamics simulation

Jingxin Wang, Chenglin Liu, Jianguo Yu *

National Engineering Research Center for Integrated Utilization of Salt Lake Resources, East China University of Science and Technology, 130 Meilong Road, 200273, Shanghai CHINA

(*Corresponding Author: Email: jgyu@ecust.edu.cn)

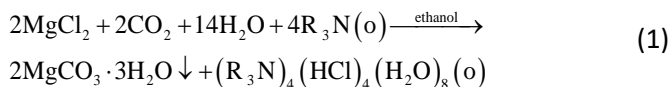
ABSTRACT

For the coupled reaction-extraction-alcohol precipitation process, it is necessary to investigate the effect of ethanol on $\text{MgCO}_3 \cdot 3\text{H}_2\text{O}$ at the molecular level. In this study, DFT calculations of the nesquehonite growth models were performed to analyze the growth unit adsorption mechanism in the presence of solvent molecules. Furthermore, molecular dynamics simulations of solid-liquid interface models and $\text{Mg}(\text{HCO}_3)_2$ solution boxes were conducted. The calculated results showed that with the ethanol effects, the adsorption rate of GU was increased by weakening competition of water molecules and the transformation rate of $\text{Mg}(\text{HCO}_3)_2$ to nesquehonite was raised by reducing the coordination number of magnesium ions.

Keywords: $\text{MgCO}_3 \cdot 3\text{H}_2\text{O}$, ethanol, CO_2 mineralization, DFT, molecular dynamics simulation

1. INTRODUCTION

Mineralizing CO_2 is an effective way to reduce the greenhouse effect. However, most CO_2 utilization projects are difficult to be commercialized due to high costs^[1]. Coupled reaction extraction alcohol precipitation process^[2] to mineralize CO_2 is an effective and achievable method, in which waste MgCl_2 and greenhouse gas carbon dioxide are transformed into high-valued magnesium carbonate and hydrogen chloride. The process mentioned above can be described by the following equation:



Nesquehonite is a naturally occurring magnesium carbonate with a chemical formula of $\text{MgCO}_3 \cdot 3\text{H}_2\text{O}$. Because of its excellent physico-chemical properties, such as non-toxicity, high physical strength and high

electrical insulation, nesquehonite is widely applied in medical, cosmetics and electronics industries^[4], etc.

As generally known, Ethanol strongly affect the morphologies of crystals and influences their phase stabilities in mixed water-ethanol solutions^[5-7]. The previous studies mainly focused on the effect of ethanol on the reaction rate and yield of crystal^[8]. However, the effect of ethanol on the morphology of the $\text{MgCO}_3 \cdot 3\text{H}_2\text{O}$ is still unclear.

In this study, the effect of ethanol on crystal growth and morphology of $\text{MgCO}_3 \cdot 3\text{H}_2\text{O}$ was investigated from the aspects of DFT calculation and molecular dynamics simulation. The main aim was to explain the growth mechanism of $\text{MgCO}_3 \cdot 3\text{H}_2\text{O}$ in the presence of ethanol at the molecular level. The results of this study would fill the gap between crystallographic characteristics and the crystal morphology.

2. EXPERIMENTAL

2.1 Materials and synthesis of $\text{MgCO}_3 \cdot 3\text{H}_2\text{O}$

Ethanol ($\geq 99.7\text{wt}\%$) and analytically pure MgCl_2 , Na_2CO_3 were purchased from Sinopharm Chemical Reagent Co., Ltd., China. CO_2 with 99.9% purity was supplied by Air Liquide (China) R&D Co., Ltd. Each experiment was conducted with deionized water.

The experimental device used in nesquehonite crystallization experiments was illustrated in Fig. 1. The

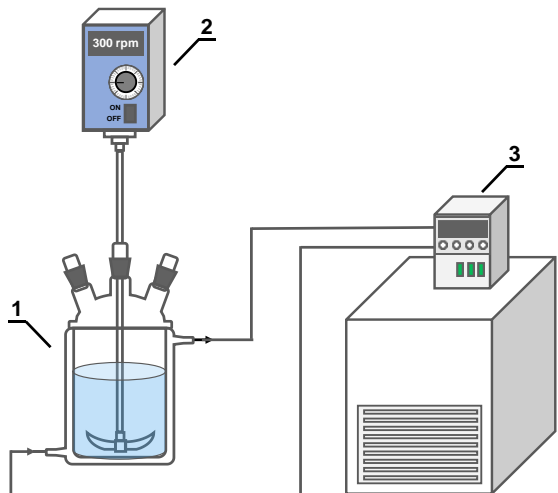


Fig. 1. Schematic illustration of the experimental device (1-jacketed reactor;2-stirrer;3- thermostatic water bath)

The Perdew-Wang's 1991 (PW91) exchange correlation function for generalized gradient approximation (GGA) in the CASTEP program of Materials Studio software was adopted to perform all the periodic DFT calculations through this work. A plane-wave cutoff energy of 540 eV was chosen for the nesquehonite DFT calculations, while Brillouin-zone integrations were sampled with k-point of a $3 \times 5 \times 2$ grid, which were the most appropriate for the system. Particularly, a set of ultrasoft pseudo-potentials designated as 00.usp were employed for H, C, O and Mg elements to describe the electron-ion interactions^[9]. For self-consistent electronic minimization, the SCF tolerance was set as "fine" with high accuracy of 1×10^{-6} eV/atom for energy convergence. Geometry structures were optimized until the changes in forces and energy less 0.05 eV/\AA and 2×10^{-5} eV/atom, respectively, in two successive iterations.

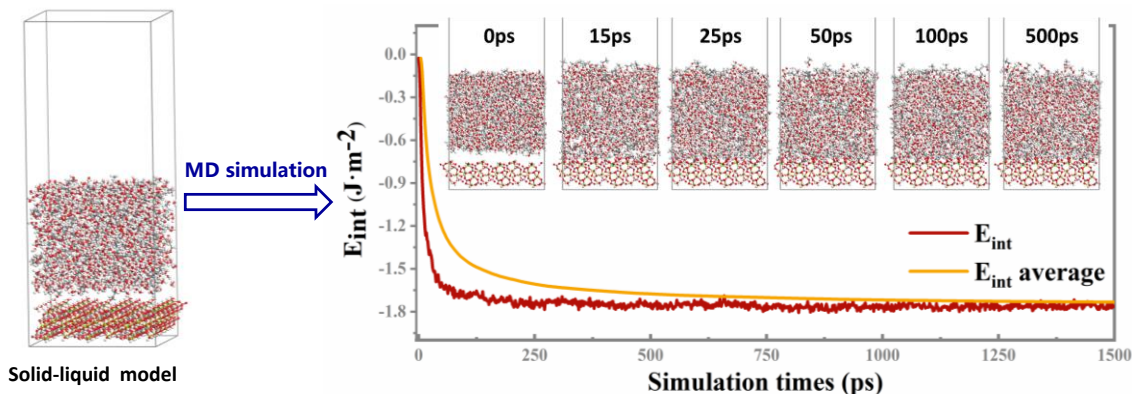


Fig. 2. Schematic representation of the solid-liquid box modeling procedure

$\text{Mg}(\text{HCO}_3)_2$ solution with a concentration of 0.20 mol/L was newly prepared for each experiment because it is unstable. First, 500 mL $\text{Mg}(\text{HCO}_3)_2$ solution was added to the jacketed reactor. The reaction temperature was controlled at 25°C by thermostatic water bath and the agitation rate was maintained at 300 rpm. Then, a certain amount of ethanol was added into the reactor rapidly. After reaction, the suspension was filtered, washed with deionized water, and dried at 40°C for 24 h.

The crystal morphology of the nesquehonite samples was obtained by using a high-resolution scanning electron microscope (SEM, Nava NanoSEM 450, FEI, USA). The crystal structures of the samples were determined by X-ray diffraction (XRD, D8 Advance, Bruker, Germany). A laser particle size analyzer (Mastersizer 3000, Malvern, England) was employed to determine the particle size of the samples.

2.2 Computational Methods

2.3 The adsorption model

Three growth surfaces of Nesquehonite slab model was optimized to calculate adsorption energies between growth unit and crystal surface both in water and in the presence of ethanol molecules. To reduce the impact of human factors and ensure an adequate distribution of the water layer and ethanol-water layer, the water layer (54 water molecules) and ethanol-water layer (54 water molecules and 13 ethanol molecules) were placed respectively on the relaxed surface of nesquehonite to construct an interface system. The molecular dynamic simulation of the interface system was carried out in Forcite module with NVT ensemble for 1500 picoseconds to ensure the surface molecules relax within the completely fixed surface. In order to save the calculation cost, only the molecules closest to the surface were retained for the following DFT calculations^[10]. Structure

of the Dominant Growth Unit of nesquehonite was obtained as described in reference^[11].

The relaxed surfaces, the closest solution molecules and the growth unit (GU) were used to construct the adsorption models. After that, the Castep tool served to optimize the structure of the adsorption models.

The binding energy of GU on the nesquehonite relaxed surface were calculated by the formula below:

$$\Delta E = E_{\text{system}} - E_{\text{GU+solution}} - E_{\text{surf+solution}} + E_{\text{solution}} \quad (2)$$

where E_{system} is the total energy of the optimized adsorption system; $E_{\text{GU+solution}}$ is the energy of growth unit and closest solution molecules; $E_{\text{surf+solution}}$ is the energy of nesquehonite relaxed surface and closest solution molecules. Note that the more negative the binding energy is, the much tighter binding between the growth unit and surface.

2.4 MD simulations

All MD simulations were performed in the Forcite program of Materials Studio software with the COMPASS II force field. The convergence level was ultrafine. Temperature and pressure were controlled using the nose method. The total energy while using the NVT ensemble was recorded to determine the equilibrium.

To illustrate the interaction mechanism between crystal surface and solvent, solid-liquid interface models (E_{total}) were built to calculate the interaction energy of water or ethanol (E_{solvent}) on the fixed supercell surface (E_{surf}), respectively. The models were relaxed by geometry optimization and NVT (1500 ps, 298.15 K) dynamic simulations. The interaction energy was determined as follows:

$$E_{\text{int}} = E_{\text{Total}} - E_{\text{solvent}} - E_{\text{surf}} \quad (3)$$

Solution simulations were carried out for $\text{Mg}(\text{HCO}_3)_2$ aqueous solutions with different ethanol concentrations. The detailed information of $\text{Mg}(\text{HCO}_3)_2$ solution boxes is shown in Table 1, which is based on real solutions. The boxes were relaxed by geometry optimization, NPT ($P = 10^{-4}$ GPa, $T = 298.15$ K, 1500 ps), and NVT (1500 ps, $T = 298.15$ K) dynamic simulations.

Table 1. Detailed information of $\text{Mg}(\text{HCO}_3)_2$ solution boxes

wt/%	Mg^{2+}	HCO_3^-	H_2O	EtOH	$\rho/\text{g}\cdot\text{mL}^{-1}$
0%	3	6	780	0	1.029
13.0%	3	6	780	33	1.005
39.0%	3	6	780	195	0.955
60.0%	3	6	780	333	0.903

The mean square displacement (MSD) for evaluating the Mg^{2+} diffusion performance was calculated by the formula below:

$$\text{MSD} = \sum_{i=1}^N \left(|r_i(t) - r_i(0)|^2 \right) \quad (4)$$

where $r_i(t)$ is the position of the i ion at time t , and $r_i(0)$ is the initial position.

The radial distribution function (RDF) between Mg

Table 3. Surface energies of different relaxed surfaces

Surface	$A/\text{\AA}^2$	Relaxed $E_{\text{surf}}(\text{J}/\text{m}^2)$
(1,0,1)	79.150	0.2376
(-1,0,1)	78.330	0.3537
(0,1,1)	102.286	0.5697

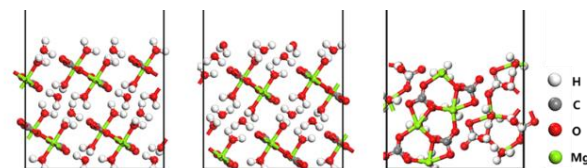


Fig. 4. Structures of different nesquehonite surfaces a-(1,0,1); b-(-1,0,1); c-(0,1,1)

ions and water molecules in the NVT frame represents the position of the different water molecules relative to the Mg ion. This could explain the influence mechanism of ethanol for the Mg ions structure of liquid at atomic level. The average number of solvent molecules around an ion in the first solvation circle is defined as the coordination number, which was calculated as follows:

$$\text{CN}(r) = \int_0^r 4\pi r^2 \rho g(r) dr \quad (5)$$

where $\text{CN}(r)$ is the average coordination number, ρ is the average number density, $g(r)$ and r represent the radial distribution function and the first peak-valley distance, respectively.

3. RESULT AND DISCUSSION

3.1 Crystal morphology of $\text{MgCO}_3 \cdot 3\text{H}_2\text{O}$

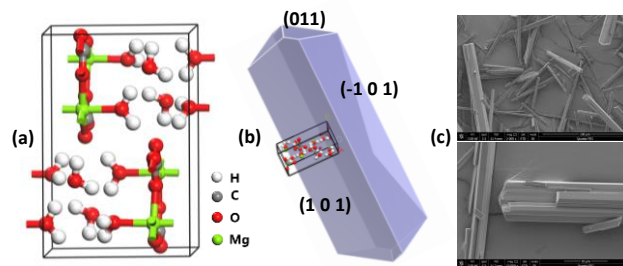


Fig. 3. (a) The lattice structure of $\text{MgCO}_3 \cdot 3\text{H}_2\text{O}$ after geometry optimization; (b) Crystal morphology of $\text{MgCO}_3 \cdot 3\text{H}_2\text{O}$ predicted by AE model. (c) SEM image of $\text{MgCO}_3 \cdot 3\text{H}_2\text{O}$ cultivated from water solvent.

The bulk crystal structure of the nesquehonite displayed in Fig.3 (a) was obtained from the American Mineralogist Crystal Structure Database (AMCSD). As can be seen from Table 2, The lattice parameters of the optimized nesquehonite structure were consistent with the experimental results^[12].

As shown in Fig.3, the crystal morphology of nesquehonite predicted by the attachment energy model (AE model) was in good agreement with the SEM

Table 2. Comparison of Experimental and optimized Lattice Parameters of $MgCO_3 \cdot 3H_2O$

Parameter	Experimental	Castep	Difference
a (Å)	7.701	7.833	1.71%
b (Å)	5.365	5.518	2.85%
c (Å)	12.126	11.928	-1.63%
β (°)	90.410	90.648	0.26%

result of nesquehonite prepared from the water solvent. The results showed that (101), (-101), and (011) were the most commonly exposed surfaces. Therefore, (101), (-101), and (011) surfaces was chosen as the further study object for following simulations.

Accordingly, the Gibbs-Curie-Wulff theorem^[13] states that the growth rate of the crystal plane is in proportion to the surface energy, and crystal morphology is determined by the slow growth rate surfaces with low surface energies. Based on the calculations presented in table 3, (011) surface has the highest surface energy expected to the fastest growth rate. (101) and (-101) surfaces are more stable than (011) surface, thus nesquehonite crystal tend to be needle-like shape.

3.2 Growth Properties of nesquehonite Surfaces in vacuum

The chemical structure of $Mg(HCO_3)_2$ in aqueous solution is $[MgHCO_3(H_2O)_4]^+$, which was calculated through first principles molecular dynamics simulations^[14]. The optimized structure of $[MgHCO_3(H_2O)_4]^+$ represents the growth unit of nesquehonite in aqueous solution.

In order to obtain the growth properties without external influence, the adsorption models of GU on nesquehonite surface in vacuum were investigated.

For (101) and (-101) surfaces, there is no exposed Mg or C atom, meaning no ionic bond could be formed between GU and surface. For the (011) surface, it has three adsorption modes. One type is that one O atom of HCO_3 (O_c) in GU is put directly above the Mg atom of the surface, while the second type is that one O atom of H_2O (O_w) in GU is placed above the Mg atom. The third type is two-point adsorption mode, which is put the GU on the

top site with its O and Mg atoms toward the Mg and O atoms of the surface, respectively.

Table 4 shows the adsorption energies of GU onto

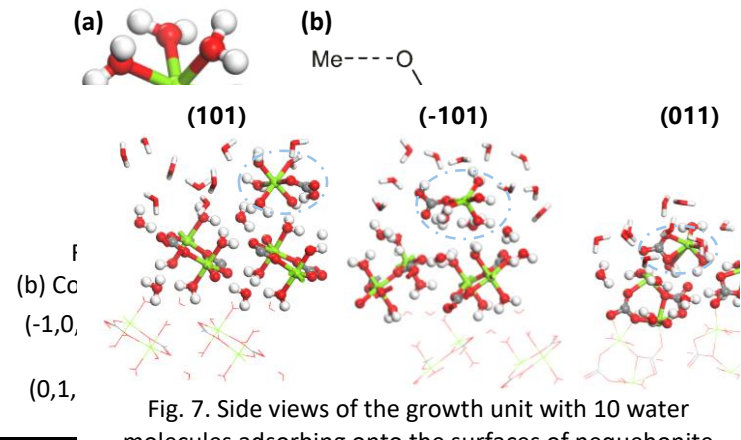


Fig. 7. Side views of the growth unit with 10 water molecules adsorbing onto the surfaces of nesquehonite

nesquehonite surfaces in vacuum. The values of E_{Total} are negative than that of the (011) surface, indicating the

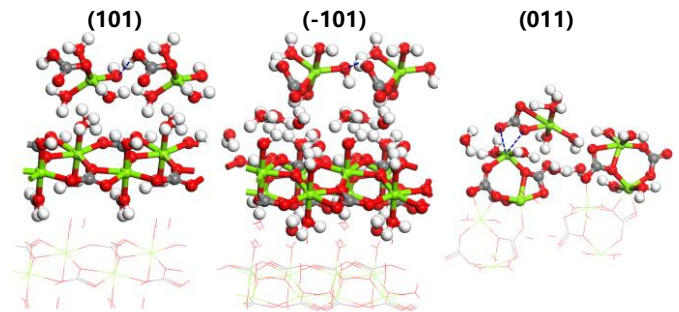


Fig. 6. Side views of the growth unit adsorbing onto the surfaces of nesquehonite

(101) and (-101) surfaces are more stable surfaces after adsorption. The double point adsorption mode of (011) surface is the dominant adsorption type because of the most negative value of ΔE_{ads} .

3.3 The Growth model with H_2O molecules

It is necessary to investigate the adsorption behaviors of GU with H_2O molecules on nesquehonite surface because the solvent effect cannot be neglected.

Table 5. Adsorption Energies of Growth Unit onto Surfaces

Surface	$H_2O \Delta E(J/m^2)$	Ethanol $\Delta E(J/m^2)$
(1,0,1)	-0.2943	-0.3324
(-1,0,1)	-0.4456	-0.6992
(0,1,1)	-0.6907	-1.0987

The adsorption energies with water molecules of the (101) and (-101) surfaces increased, while the (011) surface was decreased compared with vacuum environment. This phenomenon might be explained by

the competitive adsorption between GU and water molecules onto (011) surface.

3.4 Growth model with ethanol and H₂O molecules

Fig.8 illustrates the adsorption behavior of GU at presence of ethanol molecules. The adsorption energies were more negative when ethanol molecules were present as a result of weakening competition of water molecules. Ethanol is a relatively low-polar solvent while water is a strong polar solvent, so the polarity of the solution will decrease continuously as ethanol is added to water^[15]. Therefore, the adsorption of GU on three nesquehonite exposed planes were enhanced and hence promotes the growth along all directions.

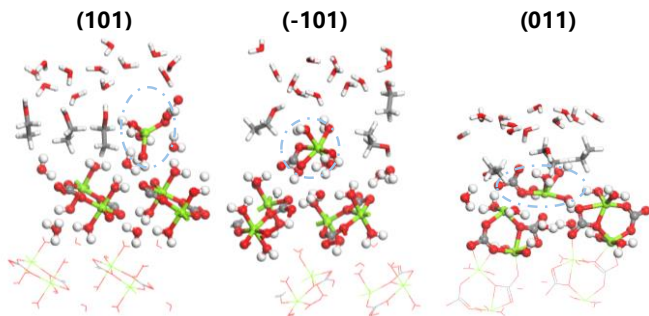


Fig. 8. Side views of the growth unit with 12 water and 3 ethanol adsorbing onto the surfaces of nesquehonite

3.5 Molecular dynamics simulation results

In order to simulate the change of solvent species, the adsorption energy of different solvent layers on the nesquehonite planes was calculated respectively by changing the proportion of ethanol (wt%=0%, 39.0%, 100.0%) in the solution layer. The specific results were displayed in Table 6. When the proportion of ethanol increased from 0% to 100%, the value of interaction energies between solvent layers and surfaces became less negative. Therefore, during the process of crystallization, it would be easier to remove solvent molecules on the crystal growth surface due to the presence of ethanol.

Table 6. Interaction Energies of between solvent and Surface

surface	$E_{int}(\text{kcal}\cdot\text{mol}^{-1}\cdot\text{\AA}^{-2})$		
	H ₂ O	0.39wt _{ethanol}	ethanol
(1,0,1)	-0.671	-0.658	-0.553
(-1,0,1)	-0.576	-0.557	-0.450
(0,1,1)	-1.825	-1.764	-0.972

Molecular dynamic (MD) simulations of different Mg(HCO₃)₂ boxes were carried out to provide mechanistic insight into the ethanol influence on Mg ions in aqueous solution.

The coordination numbers of Mg-O (oxygen in water) in ethanol-water mixtures obtained by radial distribution function analysis are shown in Fig. 9.

For pure water solution, the coordination number in the first solvation circle of Mg ions is 6, which is consistent with experimental results^[16], indicating that the molecular dynamics method adopted in this paper is reliable. when the mass fraction of ethanol increases from 13.0% to 60.0%, the coordination number decreases from 5.66 to 4.33. In conclusion, the addition of ethanol increases the transformation rate of Mg(HCO₃)₂ to nesquehonite by reducing the coordination number of magnesium ions.

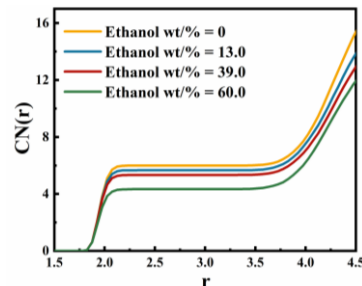


Fig. 9. The running coordination number in solution.

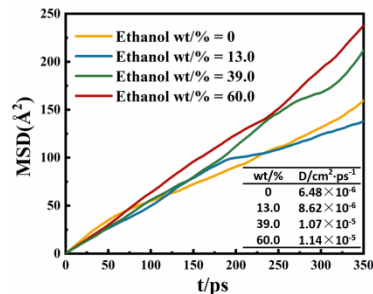


Fig. 10. MSD analysis of Mg ions in different solutions

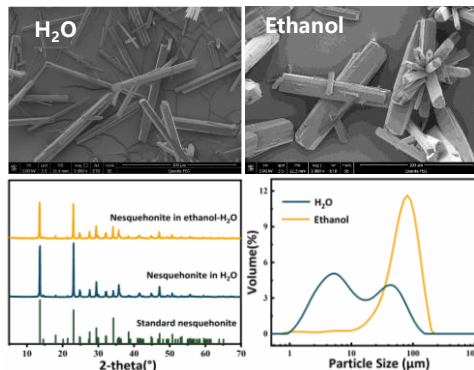


Fig. 11. SEM, XRD and particle size of nesquehonite

Fig.10 shows the mean square displacement (MSD) of Mg²⁺ in aqueous solutions with different ethanol concentrations. The red line (wt%=60.0%) shows the highest MSD values, corresponding to the highest diffusion coefficient within the time interval (350 ps). Meanwhile, changes in the diffusion coefficients of Mg²⁺ derived from the MSD data for high-concentration

ethanol solution (wt% >40.0%) are small (red and green lines, respectively), reflecting higher concentration had limited positive effect.

4. CONCLUSIONS

The influence of ethanol on crystal growth and morphology of $\text{MgCO}_3 \cdot 3\text{H}_2\text{O}$ was investigated through DFT and MD simulations. The experimental results showed that the particle size of $\text{MgCO}_3 \cdot 3\text{H}_2\text{O}$ was increased in the presence of ethanol. The first principle DFT calculations further reveals that the GU in form of $[\text{MgHCO}_3(\text{H}_2\text{O})_4]^+$ is the favorable adsorption configuration on nesquehonite (011) surface. In addition, GU adsorbed on the hydration surface of nesquehonite (011) more strongly than that without ethanol molecules. The MD simulation results of surface interaction energy, radial distribution function and mean square displacement show that the existence of ethanol improve the transformation rate of $\text{Mg}(\text{HCO}_3)_2$ to nesquehonite by reducing the coordination number and improve the diffusion coefficient of magnesium ions, respectively. Those findings could provide theoretical foundations for the coupled reaction-extraction-alcohol precipitation process to fix CO_2 .

ACKNOWLEDGEMENT

The work was supported by the Key Research and Development Program of Jiangxi Province (20223BBG74008); ECUST-Jinghao Salt Chemical Joint Research Centre of Carbon and Calcium Cycles.

DECLARATION OF INTEREST STATEMENT

The authors declare that they have no known competing financial interests or personal relationships that could have appeared to influence the work reported in this paper. All authors read and approved the final manuscript.

REFERENCE

[1] Liu S Y, Cai G H, Cao J J, et al. Influence of soil type on strength and microstructure of carbonated reactive magnesia-treated soil[J]. *European Journal of Environmental and Civil Engineering*, 2020, 24(2): 248-266.
[2] McCutcheon J, Power I M, Shuster J, et al. Carbon sequestration in biogenic magnesite and other magnesium carbonate minerals[J]. *Environmental Science & Technology*, 2019, 53(6): 3225-3237.
[3] Chen G, Song X, Dong C, et al. Mineralizing CO_2 as $\text{MgCO}_3 \cdot 3\text{H}_2\text{O}$ using abandoned MgCl_2 based on a coupled reaction-extraction-alcohol precipitation process[J]. *Energy & Fuels*, 2016, 30(9): 7551-7559.

[4] Hornak J. Synthesis, properties, and selected technical applications of magnesium oxide nanoparticles: A Review[J]. *International Journal of Molecular Sciences*, 2021, 22(23): 12752-12763.
[5] Sand K K, Rodriguez-Blanco J D, Makovicky E, et al. Crystallization of CaCO_3 in water-alcohol mixtures: Spherulitic growth, polymorph stabilization, and morphology change[J]. *Crystal Growth & Design*, 2012, 12(2): 842-853
[6] Cheng W T, Zhang C Y, Cheng H G, et al. Effect of ethanol on the crystallization and phase transformation of $\text{MgCO}_3 \cdot 3\text{H}_2\text{O}$ in a $\text{MgCl}_2\text{-CO}_2\text{-NH}_3 \cdot \text{H}_2\text{O}$ system[J]. *Powder Technology*, 2018, 335: 164-170.
[7] Li J, Zhang S, Gou R, et al. The effect of crystal-solvent interaction on crystal growth and morphology[J]. *Journal of Crystal Growth*, 2019, 507: 260-269.
[8] Song X, Dai C, Chen G, et al. Effect of alcohol on the crystallization process of $\text{MgCO}_3 \cdot 3\text{H}_2\text{O}$: An experimental and molecular dynamics simulation study[J]. *Energy Sources, Part A: Recovery Utilization and Environmental Effects*, 2019, 42(9): 1118-1131.
[9] Lu S, Yan P, Gao Y, et al. Insights into the structures, energies and electronic properties of nesquehonite surfaces by first-principles calculations[J]. *Advanced Powder Technology*, 2020, 31(8): 3465-3473.
[10] Hu Y, He J, Zhang C, et al. Insights into the activation mechanism of calcium ions on the sericite surface: A combined experimental and computational study[J]. *Applied Surface Science*, 2018, 427: 162-168.
[11] Lu S, Yan P, Gao Y, et al. Theoretical investigation of the energies, structures, and growth properties of hydromagnesite surfaces[J]. *Crystal Growth & Design*, 2020, 20(6): 3722-3731.
[12] G. Giester, C.L. Lengauer, B. Rieck, The crystal structure of nesquehonite, $\text{MgCO}_3 \cdot 3\text{H}_2\text{O}$, from Lavrion, Greece, *Mineralogy and Petrology*, 70(2000), 153–163.
[13] Li R J, Zhang X T, Dong H L, et al. Gibbs-curie-wulff theorem in organic materials: A case study on the relationship between surface energy and crystal growth[J]. *Advanced Materials*, 2016, 28(8): 1697-1702.
[14] Di Tommaso D, de Leeuw N H. First principles simulations of the structural and dynamical properties of hydrated metal ions Me^{2+} and solvated metal carbonates ($\text{Me} = \text{Ca}, \text{Mg}$, and Sr)[J]. *Crystal Growth & Design*, 2010, 10(10): 4292-4302
[15] Li Y J, Fu X T, Duan D L, et al. Extraction and identification of phlorotannins from the brown alga, *sargassum fusiforme* (harvey) setchell[J]. *Marine Drugs*, 2017, 15(2), 49.
[16] Wu XJ, and Chen XL. Study on the infrared spectra of ethanol under action of Mg^{2+} [J]. *Chemistry*, 2009, 72(6): 561-64.